

# Nanoscale radius-graded photonic crystal sensor arrays using interlaced and symmetrical resonant cavities for biosensing



Qi Liu<sup>a</sup>, Huiping Tian<sup>a,\*</sup>, Daquan Yang<sup>a,b</sup>, Jian Zhou<sup>a</sup>, Yi Yang<sup>a</sup>, Yuefeng Ji<sup>a</sup>

<sup>a</sup> The State Key Laboratory of Information Photonics and Optical Communications, School of Information and Telecommunication Engineering, Beijing University of Posts and Telecommunications, Beijing 100876, China

<sup>b</sup> School of Engineering and Applied Science, Harvard University, Cambridge, MA 02138, USA

## ARTICLE INFO

### Article history:

Received 17 January 2014

Received in revised form 18 April 2014

Accepted 19 April 2014

Available online 27 May 2014

### Keywords:

Photonic crystal

Biosensor

Nanocavity

Waveguide

Integrated optics devices

## ABSTRACT

In this work, we propose radius-graded photonic crystal sensor arrays applied on nano-scale optical platform for label-free biosensing. Two L3 cavities and two H1 cavities are multiplexed and interlaced on both sides of a photonic crystal W1 waveguide on the radius-graded photonic crystal slab. The optical sensing characteristics of the nanocavity structure are predicted by three-dimensional finite difference time domain (3D-FDTD) simulation. In response to the refractive index change of air holes surrounding the cavities, four interlaced and symmetrical cavities are shown to independently shift their resonant wavelength without crosstalk. The simulation results demonstrate the refractive index sensitivity of sensor array varies from 66.67 to 136.67 nm/RIU corresponding to the number of functionalized air holes ranged from 4 to 21. This design makes different cavities multiplexed on both sides of waveguide possible. Meanwhile, the radius-graded photonic crystal with more symmetrical and interlaced cavities is better for large integration in the sensor arrays.

© 2014 Elsevier B.V. All rights reserved.

## 1. Introduction

Since E. Yablonovitch and S. John firstly introduced the concept of photonic bandgap (PBG) in 1987 [1,2], photonic crystal (PhC) has attracted increasing attention in the past decades. Due to wide photonic bandgap and photon confinement ability, PhC devices are applied in many fields (e.g., photonic crystal filters [3–9], electro-optical modulators [10–12], switching devices [13,14], and delay devices [15]). Besides, PhC sensors seem to be very promising because of their ultracompact size, high spectral sensitivity and more suitable for monolithic integration. Thus, during the last decades, many PhC sensors for different sensing applications have been demonstrated, such as stress sensing, humidity sensing, refractive index sensing, and biochemical sensing [16–23].

With the extensive research about photonic crystal sensors, ultra-high quality factor (Q) and high sensitivity can be achieved by using different kinds of structures such as microcavities [24,25], resonant rings and disks [26], slot waveguides [27,28], and heterostructures [29]. Photonic crystal biosensors detect analyte

attached to the surface (surface-based sensing) or liquids filled into the holes around the PhC (bulk index sensing) via modulation of microcavity resonant wavelength. When the molecule exposed to a photonic crystal sensor is changed, the effective refractive index of the cavities will be changed. According to the Bragg diffraction principle [41], the resonant wavelength will shift along with the change of refractive index based on the same structure. So, a shift in the resonant wavelength peak will be caused in the transmission spectrum. Here the magnitude of the resonant wavelength shift is related to many factors, such as the number of functionalized holes, the spatial overlap of the mode with the analyte, the bandwidth of the photonic crystal structure, and so forth. Recently, nanoscale photonic crystal sensor array has drawn much attention. The photonic crystal sensor arrays make detecting different analyte simultaneously on a single platform possible. Considering the multiple sensing performance and label-free biomolecular detection, photonic crystal sensor array is a better choice. Examples of such structures include that Yang et al. demonstrated a nanoscale photonic crystal sensor array on monolithic substrates using side-coupled resonant cavity arrays [30], S. Pal et al. designed a multiple nanocavity coupled device for error-corrected optical biosensing [31], and S. Mandal et al. proposed a nanoscale optofluidic sensor array based on a silicon waveguide with 1D (one dimensional) photonic crystal microcavity [32]. However, the drawbacks of these sensor arrays are that the scale is larger and

\* Corresponding author at: Beijing University of Posts and Telecommunications, P.O. BOX 90, #10 Xitucheng Road Haidian District, Beijing 100876, China. Tel.: +86 10 62282153.

E-mail addresses: [hptian@bupt.edu.cn](mailto:hptian@bupt.edu.cn) (H. Tian), [jyf@bupt.edu.cn](mailto:jyf@bupt.edu.cn) (Y. Ji).

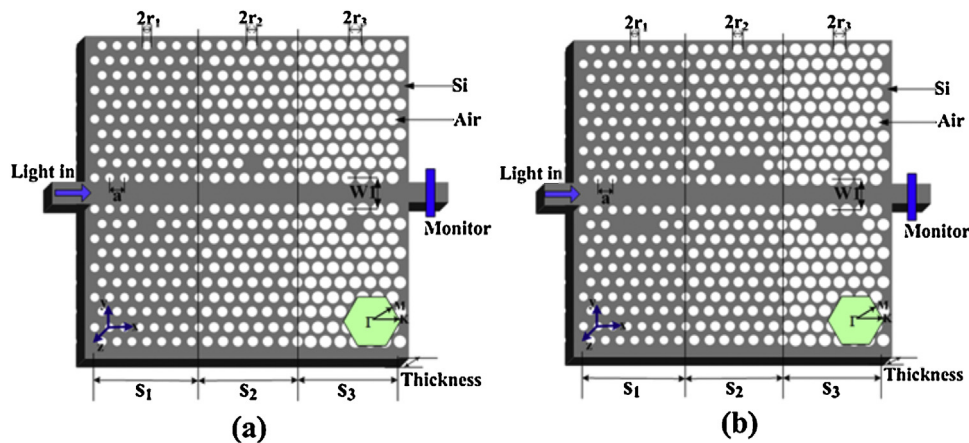


**Fig. 1.** 3D illustration of the graded photonic crystal with interlaced micro-cavities, where  $a = 437$  nm,  $T = 0.5a$ ,  $r_1 = 0.28a$ ,  $r_2 = 0.3a$ ,  $r_3 = 0.32a$ . (a) structure for H1 cavity; (b) structure for L3 cavity.

fewer cavities could be allowed without crosstalk due to the limited bandwidth.

In this work, we propose a novel ultracompact interlaced and symmetrical radius-graded photonic crystal sensor array which can overcome the above limitations. The radius-graded photonic crystal structure has drawn much attention for some years. Works have mainly focused on the electromagnetic waves which propagate and transform along the graded structure. Due to its ability to efficiently control the propagation of light, the graded photonic crystal has been successfully applied as light bending, lens and photonic crystal demultiplexer [33–40]. In this paper, we firstly introduce the radius-graded structure to design photonic crystal sensor arrays. The device contains two pairs of interlaced and symmetrical resonant cavity arrays side-coupled to PhC W1 waveguide. Considering the easier and more accurately design in practical applications, we choose L3 cavity and H1 cavity as the resonant cavities [42–44,19,45]. By using three-dimensional finite-difference time-domain (3D-FDTD), we optimize the distance between the two cavities to minimize the size of photonic crystal sensor arrays without crosstalk. The sufficient simulation results reveal that the resonant wavelength of each micro-cavity shift linearly when the effective refractive index around the cavity change. The radius-graded photonic crystal sensor arrays can detect different kinds of analyte at the same time. In addition, the total sensor sensitivity is 113.34 nm/RIU as the functionalized holes equal 12 ( $N = 12$ ). If we change the number of functionalized air holes, the sensitivity varies from 66.67 nm/RIU ( $N = 4$ ) to 136.67 nm/RIU ( $N = 21$ ). In addition, if we only use L3 cavity as the interlaced resonant cavity, the number of the microcavities could be added to six along with the direction of radius increasing in the platform. This means that the structure based on the nanoscale radius-graded photonic crystal platform is promising in the optical integrated circuit in the future.

## 2. Design of the radius-graded photonic crystal with interlaced micro-cavities

We examine the effect of adding different microcavities (H1 or L3) to the radius-graded photonic crystal sensor arrays by performing 3D-FDTD simulations. The 3D illustration of our radius-graded photonic crystal sensor arrays structure with three interlaced H1 and L3 microcavities are shown in Fig. 1(a) and (b), respectively. The PhC devices have lattice constants ( $a$ ) of 437 nm with a slab thickness of  $0.5a$  (220 nm). Additionally, the structure in our paper is designed on a silicon slab ( $n_{Si} = 3.48$ ) by arranging a triangular lattice of air holes. Moreover, the radius in our design is graded with  $r_1 = 0.28a$ ,  $r_2 = 0.3a$ , and  $r_3 = 0.32a$ . Using the radius-graded

photonic crystal structure, we can easily achieve microcavity arrays in a platform.

As shown in Fig. 1, H1 and L3 cavities are regarded as the resonant cavities separately. H1 cavity represents removing one air hole, and L3 cavity stands for three air holes losing. Fig. 1(a) shows the interlaced H1 microcavities, while Fig. 1(b) is the structure of L3 microcavities. The photonic crystal slab structure designed for biosensing is based on silicon, and consists of a  $21 \times 21$  array of air holes in a triangular-lattice pattern. We use the TE polarized Gaussian-pulse source as the incident source. The simulations are performed by using Meep [30] to observe the steady state electric field and the transmission spectra. For improving accuracy in the simulation, FDTD analysis of photonic crystal structure is carried out with a mesh size of  $a/200$  and time step of  $0.025a/c$ , where  $a$  is the lattice constant. All the simulations are carried out with the same mesh size and time step for future comparable results. Since the boundary conditions at the spatial edges of the computational domain must be carefully considered. The simulation area in our paper is surrounded by one-spatial unit thick perfectly matched layer (PML), in which both electric and magnetic conductivities are introduced in such a way that the wave impedance remains constant, absorbing the energy without inducing reflections. Furthermore, the structural and simulation parameters keep the same except for cavities in the future research.

Since the graded photonic crystal has been applied as demultiplexer before [35], we firstly introduce this theory to sensor arrays. Fig. 2 shows the band diagram of a W1 PhC slab waveguide by using plane wave expansion (PWE) method. From the simulation, we conclude the effective working frequency of the waveguide within the PBG is between  $0.259(2\pi c/a)$  and  $0.308(2\pi c/a)$ . In Fig. 2(a) there are three different color lines (blue, green and black) which represent the mode under conditions of different radii. We focus on the even mode in our following research. We calculate that the blue line signifies the mode in  $r = 0.28a$ , while the black one shows the mode when  $r$  is equal to  $0.32a$ . It means that as the radius increasing the guided modes move to the higher frequency (blue line to the black line). Fig. 2(b) shows the transmittance of the interlaced L3 cavities. The resonant frequency peaks of the L3 cavities all intersect with the even mode line in the band diagram. Because the radius-graded photonic crystal disrupts the periodicity, the transmission has some fluctuation on the edge of the bandgap. As seen, the radius-graded photonic crystal with three interlaced microcavities can generate three resonant wavelengths easily.

As concluded from the simulation about the structures pictured in Fig. 1, the resonant frequencies of three interlaced cavities separate clearly in the transmission spectra. To ensure every resonant

Download English Version:

<https://daneshyari.com/en/article/737054>

Download Persian Version:

<https://daneshyari.com/article/737054>

[Daneshyari.com](https://daneshyari.com)